JCTC Journal of Chemical Theory and Computation

Article

pubs.acs.org/JCTC

Are Protein Force Fields Getting Better? A Systematic Benchmark on 524 Diverse NMR Measurements

Kyle A. Beauchamp,[†] Yu-Shan Lin,[‡] Rhiju Das,[†,§] and Vijay S. Pande[†,‡,*]

[†]Biophysics Program, [‡]Chemistry Department, Stanford University, Stanford, California, United States

[§]Biochemistry Department, Stanford University, Stanford, California, United States

Supporting Information

ABSTRACT: Recent hardware and software advances have enabled simulation studies of protein systems on biophysically relevant time scales, often revealing the need for improved force fields. Although early force field development was limited by the lack of direct comparisons between simulation and experiment, recent work from several laboratories has demonstrated direct calculation of NMR observables from protein simulations. Here, we quantitatively evaluate 11 recent molecular dynamics force fields in combination with 5 solvent models against a suite of 524 chemical shift and J coupling ($^3JH_NH_\alpha$, $^3JH_NC_\beta$, $^3JH_\alpha C'$, $^3JH_NC'$, and $^3JH_\alpha N$) measurements on dipeptides, tripeptides, tetra-alanine, and ubiquitin. Of the force fields examined (ff96, ff99, ff03, ff03*, ff03w, ff99sb*, ff99sb-ildn, ff99sb-ildn-phi, ff99sb-ildn-NMR, CHARMM27, and OPLS-AA), two force fields (ff99sb-ildn-phi, ff99sb-ildn-NMR) combining recent side chain and backbone torsion modifications achieved high accuracy in our benchmark. For the two optimal force fields, the calculation error is comparable to the uncertainty in the experimental comparison. This observation suggests that extracting additional force field improvements from NMR data may require increased accuracy in J coupling and chemical shift prediction. To further investigate the limitations of current force fields, we also consider conformational populations of dipeptides, which were recently estimated using vibrational spectroscopy.

1. INTRODUCTION

Molecular dynamics (MD) simulation is a versatile computational tool that allows investigation of condensed phase systems including neat alkanes,[1] the many phases of water,[2] the solvation and binding of small molecules,[3,4] and the folding dynamics of full protein systems.[5,6] Recent gains in computer performance, parallelized MD codes,[7] and optimizations for graphics processing units[8] and other specialized hardware[9] have enabled simulations of aqueous macromolecules over times exceeding 100 ns in single-day calculations. These accelerations, however, have begun to reveal inaccuracies in current MD force fields.

By and large, molecular dynamics force fields are parametrized to reproduce quantum mechanical calculations on small model systems,[10−13] then adjusted to provide improved agreement with higher-quality ab initio data,[14] crystallographic structures,[15] or experimental data.[16−18] Because of the many design choices inherent in parametrization, force fields yield considerable differences in predicted biophysical properties. For example, studies of protein folding have revealed variation in folding rates between different force fields.[19] Similarly, simulated proteins often have folding midpoint temperatures that err by 25 K or more.[6]

Here, we systematically evaluate 11 recent force fields combined with each of five widely used water models (55 combinations) against a benchmark set of 524 NMR measurements. The evaluated force fields include recent AMBER, CHARMM, and OPLS-AA variants; the solvent models include recent implicit and explicit models. The 524 NMR measurements include J coupling and chemical shift data of 32 model systems. Measurements span all 19 nonproline amino acids and include dipeptide,[20,21] tripeptide,[22,23] tetrapeptide,[22] and full protein systems;[24] importantly, this systematic benchmark contains model systems not previously considered in the parametrization of the tested force fields. These comparisons, which comprise over 25 μs of aggregate simulation, suggest that explicit solvent simulations with either the ff99sb-ildn-phi or ff99sb-ildn-NMR force field recover NMR observables with an accuracy close to the systematic uncertainty inherent in current models for calculating scalar couplings and chemical shifts. In addition to quantitative comparisons to NMR experiments, we also compare conformational populations of the 19 dipeptides to recent estimates made using vibrational spectroscopy.[20,21]

2. METHODS

2.1. Benchmark Systems. For our benchmark, we selected 32 protein systems including capped dipeptides (Ace-X-NME, X ≠ P), tripeptides (XXX, GYG, X ∈ {A,G,V}, Y ∈ {A,V,F,L,S,E,K,M}), alanine tetrapeptide, and ubiquitin. Each of these systems has NMR data available in the form of chemical shifts, J couplings, or both. Small peptides provide minimal model systems for sampling the (ϕ,ψ) torsions that are a key component of secondary structure formation. On the other hand, a different balance of forces is at play in larger systems, which led us to include ubiquitin, a key model system in protein folding[25] and NMR studies.[24]

2.2. Force Field Benchmark. We aggregated 524 measurements of chemical shifts and scalar couplings, summarized in Table S1. Data were taken from the BioMagRes Database[26] and several recent papers.[20,22,23] Each of the 32 systems was simulated using Gromacs 4.5.4[7] using all combinations of the

Received: November 3, 2011
Published: March 12, 2012

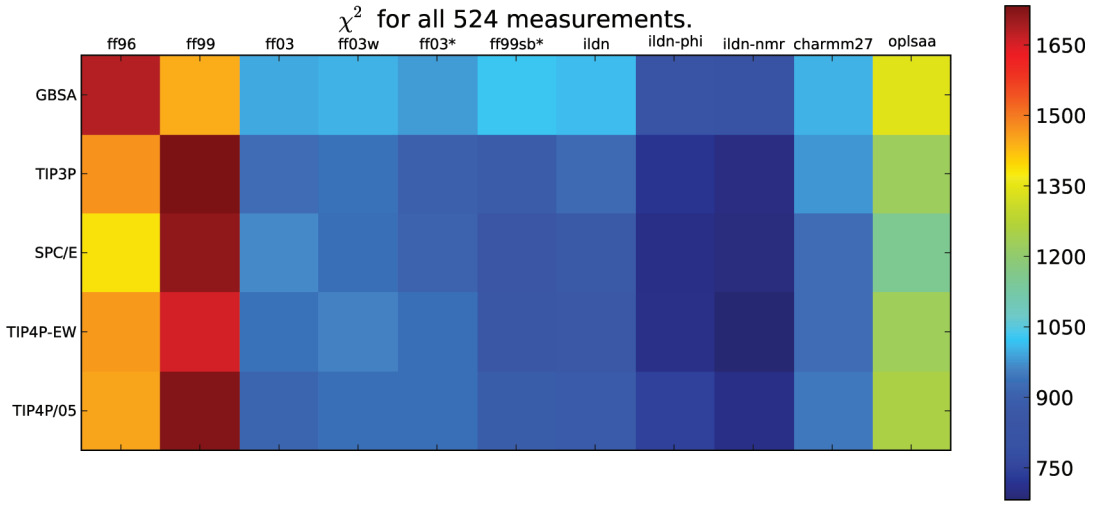

Figure 1. Force field evaluation based on all available data. The overall χ^2 quantifies the agreement with all 524 experimental measurements.

GBSA,[27] TIP3P, SPC/E, TIP4P-EW,[28] and TIP4P/2005[2] water models with the ff96,[10] ff99,[11] ff03,[12] ff03w,[16] ff03*,[17] ff99sb*,[17] ff99sb-ildn,[14] ff99sb-ildn-phi,[18] ff99sb-ildn-NMR,[29] CHARMM27,[30,31] and OPLS-AA[32] force fields. Here, ff99sb-ildn-phi refers to a force field combining the ff99sb-ildn side chain optimizations[14] with a recently modified ϕ' potential.[18] Compared to ff99sb-ildn, ff99sb-ildn-phi differs by a modification of the periodicity two ($n = 2$) ϕ' torsional potential; this term has a strength of 2.00 and 1.80 kcal/mol, respectively, for the ff99sb-ildn and ff99sb-ildn-phi force fields. The ff99sb-ildn-NMR force field refers to the combination of the ff99sb-ildn side chain optimizations with the NMR-optimized backbone torsions of the ff99sb-NMR force field.[29]

Each production simulation was 25 ns (20 ns for dipeptides) in length and held at constant temperature and pressure; simulations for peptides were started from conformations generated by PyMol. Ubiquitin simulations were started from the crystal structure (PDB: 1UBQ).[33] For error analysis, simulations were repeated with independent starting velocities. For the peptide systems, the independent runs also used different starting conformations; for ubiquitin, the second set of runs began from the crystal structure, had independent starting velocities, and were 50 ns in length. J couplings were estimated using empirical Karplus relations parametrized by Bax and Hu;[34] chemical shifts were estimated using the Sparta+ program[35] (in Figure S1, we consider alternative models for J couplings and chemical shifts).

All simulations were performed with Gromacs[7] 4.5.4. Starting conformations were solvated, neutralized with Na^+ or Cl^-, minimized, and equilibrated before production runs. For explicit solvent, electrostatics were treated using the particle mesh Ewald[36] method with a real-space cutoff of 1.0 nm. van der Waals interactions were switched off between 0.7 and 0.9 nm. Temperature control was achieved using the velocity rescaling thermostat.[37] Pressure control (1 atm) was achieved using either the Berendsen barostat (for equilibration) or the Parrinello–Rahman[38] barostat (for production). For implicit solvent simulations (GBSA), temperature control was achieved using a Langevin integrator. The temperatures were chosen to match experimental conditions; dipeptides were held at 303 K, GXG tripeptides at 298 K, homotripeptides at 300 K, and ubiquitin at 303 K. For ubiquitin, the protein was held fixed during the minimization and equilibration steps.

3. RESULTS

3.1. Optimal Performance from ff99sb-ildn-NMR and ff99sb-ildn-phi. Converting all 524 measurements into an uncertainty-weighted objective function ($\chi^2 = \sum_i (x_i^{\mathrm{Expt}} - x_i)^2/\sigma_i^2$) allows a force field evaluation based on all available data (Figure 1). We estimate the errors in each comparison as the uncertainty in the relationship between conformation and NMR observable; these errors (Tables S2 and S3) were previously determined during the parametrizations of the various Karplus relations and the Sparta+ chemical shift model. On the basis of this analysis, the early (ff96, ff99) force fields are easily rejected in favor of more recent modifications. Furthermore, ff99sb-ildn-NMR and ff99sb-ildn-phi most accurately recapitulate the chosen NMR experiments. Raw data for TIP4P-EW with several force fields are shown in Figures S4–S13.

3.2. Accuracy for Dipeptides, Tripeptides, Tetrapeptides, and Ubiquitin. The model systems in this work consist of ubiquitin, alanine tetrapeptide, tripeptides, and the 19 capped dipeptides (e.g., Acetyl–Ala–N–methylamide). Because these systems differ considerably in size, it is important to ask whether force fields perform well for all classes of model system. In particular, it is important to avoid overfitting to experiments probing only small systems, as that could compromise accuracy on larger systems where less protein is solvent-exposed. We find that ff99sb-ildn-phi and ff99sb-ildn-NMR provide good performance for all three classes of systems (Figure 2).

3.3. Performance by Experiment. For five out of 10 experiments, ff99sb-ildn-phi and ff99sb-ildn-NMR achieve accuracy comparable to the uncertainty of the comparison (e.g., $x^2/n \approx 1$; see Table S4, Figures S14–S23). Moderate deviations are found for two experiments ($^3J(H^NC')$, $^3J(H^\alpha N)$), but large deviations are found for carbonyl chemical shifts ($CS-C$), $^3J(H^\alpha C')$, and $^3J(H^NH^\alpha)$. First, large errors in carbon chemical shifts are found for all choices of force field and water model. This error may indicate systematic error in either the chemical shifts estimated by Sparta+ or the conformational propensities of *all* force fields evaluated here. Because Sparta+ is parametrized empirically using a neural network approach, it is challenging to further dissect errors in chemical shift predictions. Second, moderate errors in $^3J(H^\alpha C')$ are observed; inspection of individual errors (Figure S24) identifies GGG as

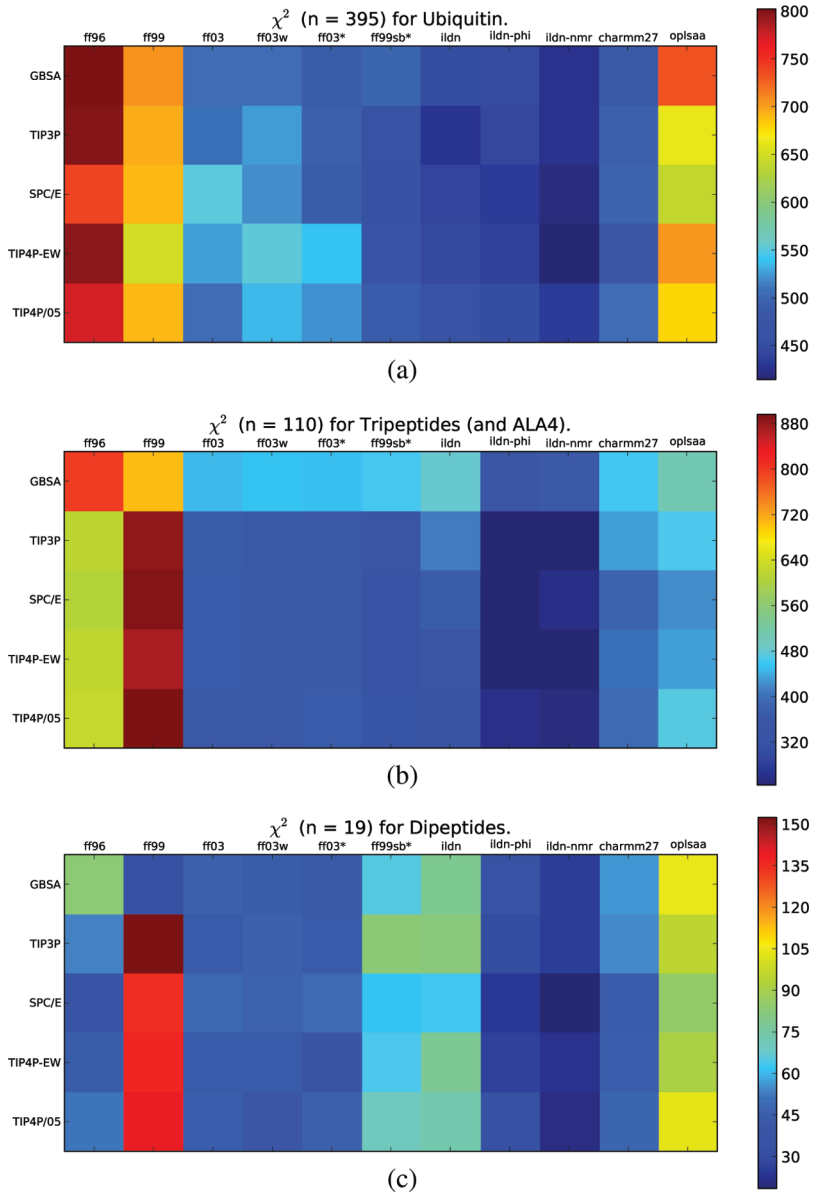

Figure 2. Accuracy for dipeptides, tripeptides, tetrapeptides, and ubiquitin. For each class of model system, χ^2 quantifies the agreement between simulation and experiment.

the largest error contributor. The failure for GGG is consistent with previous observations[18] that improved Karplus parametrizations may be required for glycine residues. Finally, moderate errors in $^3J(H^NH^\alpha)$ are observed. However, ff99sb-ildn-phi and ff99sb-ildn-NMR perform significantly better than their predecessors ff99sb-ildn and ff99 (Figure 3). The $^3J(H^NH^\alpha)$ analysis suggests that correcting backbone torsions[16−18,29] has led to real improvements in force field accuracy.

3.4. Performance By Amino Acid. Another key question is whether force field performance is consistent among the different amino acids. Large variations in quality between different amino acids might indicate a straightforward way to improve force fields. To formalize the agreement with experiment, we calculate values of reduced χ^2 (Figure 4). Values of (χ^2/n) under 1 suggest that errors are within the measurement uncertainty. This analysis leaves 6/19 amino acids open to further optimization, including ALA, GLY, SER, VAL, ILE, and ASP. Force field improvements for these residues could lead to reduced errors in the present benchmark. For the remaining amino acids, improved accuracy in chemical shift and J coupling estimation may eventually reveal force field inadequacies that are within the uncertainty of the present comparison.

3.5. Populations of 19 Dipeptides. A recent analysis[21] used NMR and vibrational spectroscopy to estimate the α_R, β, and P_{II} populations of 19 capped dipeptides. Here, we use (ϕ,ψ) state definitions[39] to estimate conformational populations from simulation (Figure 5, Figure S25). Because of uncertainties in state definitions and the fitting procedure used in the experimental analysis,[21] this comparison is less direct than the NMR comparisons above; despite this limitation, population analysis provides several insights.

First, with the exception of ff96, the MD force fields uniformly *over*-emphasize α_R in dipeptide simulations. Second, the GBSA implicit solvent model aggravates this error, leading to even further bias toward helical conformations. Third, recent force fields (ff03*, ff99sb-ildn, ff99sb-ildn-phi, ff03w, ff99sb-

dx.doi.org/10.1021/ct2007814 | J. Chem. Theory Comput. 2012, 8, 1409−1414

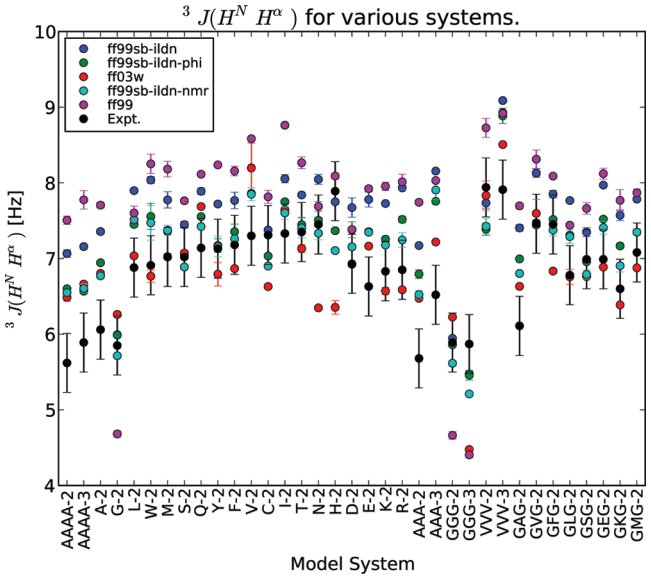

Figure 3. Performance by experiment. The errors in $^3J(H^NH^\alpha)$ suggest that the ff99sb-ildn-phi and ff99sb-ildn-NMR force fields correct a significant bias in the ϕ potential of the ff99sb-ildn force field. Values are shown for TIP4P-EW.

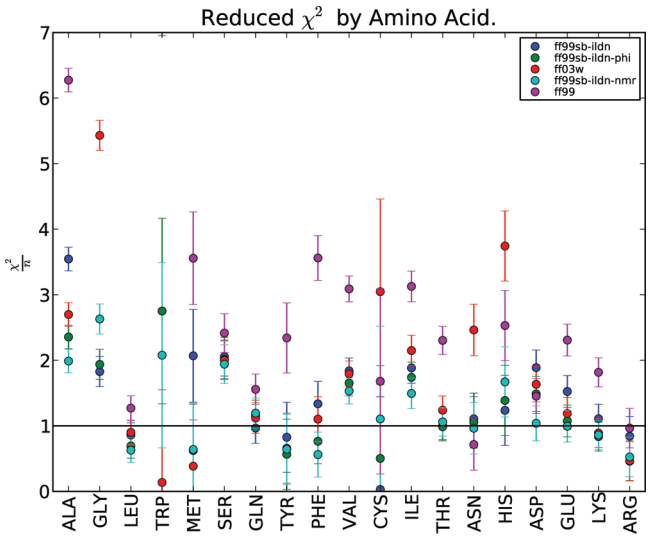

Figure 4. Calculated values of reduced χ^2. Reduced χ^2 is shown for all 19 amino acids, indicating force field quality as a function of individual amino acid. Values are shown for TIP4P-EW with five well-performing force fields. Reduced χ^2 values near 1 indicate that force field error is comparable to the experimental uncertainty, while values much larger than 1 indicate possible room for force field improvements. Errors for reduced χ^2 are given by $(2/n)^{1/2}$, where n is the number of measurements available for that amino acid. Plotted error bars underestimate the true error, as error estimates include only the contribution of the Karplus and chemical shift prediction. This contribution tends to be the dominant source of error in the present benchmark.

ildn-NMR) combined with explicit solvent show close agreement with the conformational populations estimated using a PDB-derived coil library.[39] This may suggest that current force fields perform better in the context of a full protein system or that direct comparison of simulation to IR-based population estimates is hindered by systematic error.

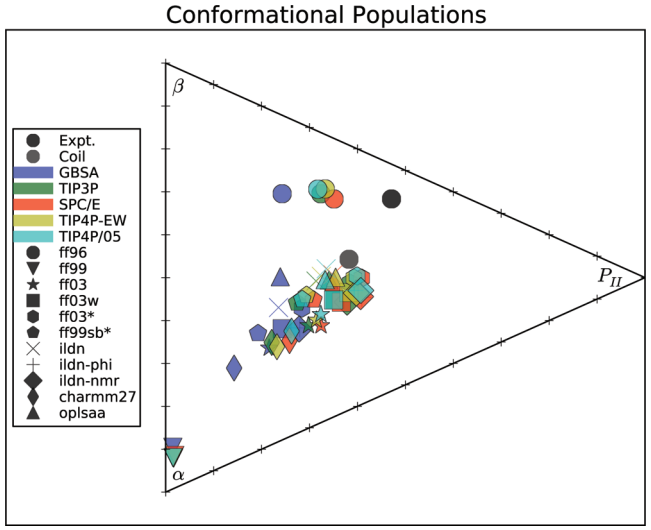

Figure 5. Estimation of conformational populations from simulation. The conformational populations for the 19 dipeptides (averaged over all 19) are shown for various force fields. Individual amino acid predictions are given in Figure S25. Grid ticks represent population increments of 0.1; the corners of the triangle represent the distributions with all β, α_R, and P_{II}, respectively. Also shown are experimental estimates[21] and statistics from a PDB-derived coil library.[39]

Although the overestimation of α_R in dipeptides suggests that further decreasing α_R may improve current force fields, such changes are not always feasible. As an example, we point out that ff99sb is known to *under*-emphasize[17] α_R in the helix-forming Ac−$(AAQAA)_3$−NH_2.[40,41] Thus, it may be challenging for fixed-charge force fields to simultaneously achieve accurate helical propensities in both dipeptide and longer protein systems. To further investigate, we simulated Ac−$(AAQAA)_3$−NH_2 using both ff99sb-ildn-phi and ff99sb-ildn-NMR (Figure S26). On the basis of this test, ff99sb-ildn-phi is somewhat underhelical, while ff99sb-ildn-NMR is somewhat overhelical. This suggests that a future modification of ff99sb-ildn-NMR with slightly reduced helical content could lead to modest improvements in force field quality.

4. DISCUSSION

4.1. Optimal Choice of Force Field and Water Model.

The overall χ^2 analysis (Figure 1) suggests that the ff99sb-ildn-phi and ff99sb-ildn-NMR force fields (with explicit water) are best able to recapitulate the 524 NMR measurements in the present benchmark. These results are robust to different models for J couplings and chemical shifts (Figure S1), to sampling uncertainty in the simulations (Figure S2), and to the relative importance placed on J coupling versus chemical shift experiments (Figure S3).

Explicit water models (TIP3P, SPC/E, TIP4P-EW, and TIP4P/2005) outperform GBSA. However, choosing between TIP3P, SPC/E, TIP4P-EW, and TIP4P/2005 is difficult, as the results are force field dependent. However, our current analysis does suggest that variants of ff99sb give reasonable performance with TIP4P-EW (and, to a lesser extent, TIP4P/2005). Recent four-point water models have improved thermodynamic properties;[2,28] our results support their broader use in protein simulations, although further testing may be necessary for benchmarking the accuracy of long-range forces.

dx.doi.org/10.1021/ct2007814 | J. Chem. Theory Comput. 2012, 8, 1409−1414

4.2. Future Force Field Development. With the simple functional forms used, how much can current force fields be improved? Given the many small but measurable improvements recently published,[14,16−18] it is likely that the current functional forms may allow further increases in accuracy. The best path for improvement, however, is complex. The nonbonded terms, including partial charges, are based on decade-old calculations; increasing computational resources allows increasingly accurate QM data to be used for parametrization. More accurate bonded terms might also be possible. Another possibility is the use of amino acid specific torsional potentials, rather than identical potentials for all (nonglycine) residues. Such a procedure would allow researchers to refine force fields for amino acids where performance is presently inadequate.

For further developments, a key question is whether to use *ab initio*[14] or experimental data[16−18,29] when fitting parameters. Fitting to *ab initio* data is hindered by the difficulty of modeling solvent effects during parametrization. Furthermore, parameters such as partial charges may not be transferable between gas and condensed phase environments—or even between hydrophobic and solvent-exposed environments. Fitting to experimental data is currently hindered by two key limitations. First, only limited data are available for model systems. Second, the quantitative connection between simulation and experiment typically relies on parametrized relationships such as the Karplus relationship or the chemical shift predictions of Sparta +. These parametrizations have large uncertainties (typically larger than the statistical errors in either simulation or experiment), may contain systematic errors (such as amino-acid specific biases[18]), and rely on protein structural models that are ensemble averaged (possibly blurring important short-time-scale dynamics[42]). The current analysis focuses on agreement with NMR (chemical shift and J coupling) experiments, which emphasize local bonded interactions. Other experimental data, such as solvation free energies, may be critical for evaluating other aspects of force field performance.

5. CONCLUSIONS

Molecular simulation promises atomic-detail modeling of key processes in chemistry and biophysics, but only if the underlying force field has demonstrated accuracy. Here, we have shown that recent force field enhancements lead to increased accuracy in recapitulating a benchmark set of 524 NMR measurements. Simulations performed in explicit water with either the ff99sb-ildn-phi or ff99sb-ildn-NMR force field achieve RMS errors that are comparable to the uncertainty in calculating the experimental observables. Future work may require advances in both force field development and accurate calculation of NMR observables.

■ ASSOCIATED CONTENT

Supporting Information

Additional error analysis is available in the Supporting Information. The Karplus relations used in this work are tabulated along with estimates of systematic uncertainty. Gromacs parameter files and PDBs for the present simulations are also included. This information is available free of charge via the Internet at http://pubs.acs.org

■ AUTHOR INFORMATION

Corresponding Author

*E-mail: pande@stanford.edu.

Notes

The authors declare no competing financial interest.

■ ACKNOWLEDGMENTS

We thank NSF CNS-0619926 for computing resources and NIH R01-GM062868, NSF-DMS-0900700, and NSF-MCB-0954714 for funding. K.A.B. was supported by a Stanford Graduate Fellowship. R.D. was supported by a Burroughs-Wellcome Foundation Career Award at the Scientific Interface. We acknowledge the following award for providing computing resources that have contributed to the research results reported within this paper. MRI-R2: Acquisition of a Hybrid CPU/GPU and Visualization Cluster for Multidisciplinary Studies in Transport Physics with Uncertainty Quantification http://www.nsf.gov/awardsearch/showAward.do?AwardNumber=0960306. This award is funded under the American Recovery and Reinvestment Act of 2009 (Public Law 111-5).

■ REFERENCES

(1) Jorgensen, W.; Maxwell, D.; Tirado-Rives, J. *J. Am. Chem. Soc.* **1996**, *118*, 11225−11236.
(2) Abascal, J.; Vega, C. *J. Chem. Phys.* **2005**, *123*, 234505.
(3) Mobley, D.; Graves, A.; Chodera, J.; McReynolds, A.; Shoichet, B.; Dill, K. *J. Mol. Biol.* **2007**, *371*, 1118−1134.
(4) Shirts, M.; Pande, V. *J. Chem. Phys.* **2005**, *122*, 134508.
(5) Beauchamp, K.; Ensign, D.; Das, R.; Pande, V. *Proc. Natl. Acad. Sci. U. S. A.* **2011**, *108*, 12734.
(6) Shaw, D. E.; Maragakis, P.; Lindorff-Larsen, K.; Piana, S.; Dror, R. O.; Eastwood, M. P.; Bank, J. A.; Jumper, J. M.; Salmon, J. K.; Shan, Y.; Wriggers, W. *Science* **2010**, *330*, 341−346.
(7) Hess, B.; Kutzner, C.; Van Der Spoel, D.; Lindahl, E. *J. Chem. Theory Comput.* **2008**, *4*, 435−447.
(8) Eastman, P.; Pande, V. *Comput. Sci. Eng.* **2010**, *12*, 34−39.
(9) Shaw, D.; Deneroff, M.; Dror, R.; Kuskin, J.; Larson, R.; Salmon, J.; Young, C.; Batson, B.; Bowers, K.; Chao, J. *Commun. ACM* **2008**, *51*, 91−97.
(10) Kollman, P. *Acc. Chem. Res.* **1996**, *29*, 461−469.
(11) Wang, J.; Cieplak, P.; Kollman, P. *J. Comput. Chem.* **2000**, *21*, 1049−1074.
(12) Duan, Y.; Wu, C.; Chowdhury, S.; Lee, M.; Xiong, G.; Zhang, W.; Yang, R.; Cieplak, P.; Luo, R.; Lee, T. *J. Comput. Chem.* **2003**, *24*, 1999−2012.
(13) Hornak, V.; Abel, R.; Okur, A.; Strockbine, B.; Roitberg, A.; Simmerling, C. *Proteins: Struct., Funct., Bioinf.* **2006**, *65*, 712−725.
(14) Lindorff-Larsen, K.; Piana, S.; Palmo, K.; Maragakis, P.; Klepeis, J.; Dror, R.; Shaw, D. *Proteins: Struct., Funct., Bioinf.* **2010**, *78*, 1950−1958.
(15) MacKerell, A. Jr; Feig, M.; Brooks, C. III. *J. Am. Chem. Soc.* **2004**, *126*, 698−699.
(16) Best, R. B.; Mittal, J. *J. Phys. Chem. B* **2010**, *114*, 14916−14923.
(17) Best, R.; Hummer, G. *J. Phys. Chem. B* **2009**, *113*, 9004−9015.
(18) Nerenberg, P.; Head-Gordon, T. *J. Chem. Theory Comput.* **2011**, *7*, 1220−1230.
(19) Piana, S.; Lindorff-Larsen, K.; Shaw, D. *Biophys. J.* **2011**, *100*, L47−L49.
(20) Avbelj, F.; Grdadolnik, S.; Grdadolnik, J.; Baldwin, R. *Proc. Natl. Acad. Sci. U. S. A.* **2006**, *103*, 1272.
(21) Grdadolnik, J.; Mohacek-Grosev, V.; Baldwin, R.; Avbelj, F. *Proc. Natl. Acad. Sci. U. S. A.* **2011**, *108*, 1794.
(22) Graf, J.; Nguyen, P.; Stock, G.; Schwalbe, H. *J. Am. Chem. Soc.* **2007**, *129*, 1179−1189.
(23) Hagarman, A.; Measey, T.; Mathieu, D.; Schwalbe, H.; Schweitzer-Stenner, R. *J. Am. Chem. Soc.* **2009**, *132*, 540−551.

(24) Wang, A.; Bax, A. *J. Am. Chem. Soc.* **1996**, *118*, 2483−2494.
(25) Krantz, B.; Sosnick, T. *Biochemistry* **2000**, *39*, 11696−11701.
(26) Ulrich, E.; Akutsu, H.; Doreleijers, J.; Harano, Y.; Ioannidis, Y.; Lin, J.; Livny, M.; Mading, S.; Maziuk, D.; Miller, Z. *Nucleic Acids Res.* **2008**, *36*, D402.
(27) Onufriev, A.; Bashford, D.; Case, D. *Proteins* **2004**, *55*, 383−394.
(28) Horn, H.; Swope, W.; Pitera, J.; Madura, J.; Dick, T.; Hura, G.; Head-Gordon, T. *J. Chem. Phys.* **2004**, *120*, 9665.
(29) Li, D.; Bruschweiler, R. *Angew. Chem.* **2010**, *122*, 6930−6932.
(30) Mackerell, A. Jr; Feig, M.; Brooks, C. III. *J. Comput. Chem.* **2004**, *25*, 1400−1415.
(31) Bjelkmar, P.; Larsson, P.; Cuendet, M.; Hess, B.; Lindahl, E. *J. Chem. Theory Comput.* **2010**, *6*, 459−466.
(32) Kaminski, G.; Friesner, R.; Tirado-Rives, J.; Jorgensen, W. *J. Phys. Chem. B* **2001**, *105*, 6474−6487.
(33) Vijay-kumar, S.; Bugg, C.; Cook, W. *J. Mol. Biol.* **1987**, *194*, 531−544.
(34) Hu, J.-S.; Bax, A. *J. Am. Chem. Soc.* **1997**, *119*, 6360−6368.
(35) Shen, Y.; Bax, A. *J. Biomol. NMR* **2010**, *48*, 13−22.
(36) Darden, T.; York, D.; Pedersen, L. *J. Chem. Phys.* **1993**, *98*, 10089.
(37) Bussi, G.; Donadio, D.; Parrinello, M. *J. Chem. Phys.* **2007**, *126*, 014101.
(38) Parrinello, M.; Rahman, A. *J. Appl. Phys.* **1981**, *52*, 7182−7190.
(39) Jha, A.; Colubri, A.; Zaman, M.; Koide, S.; Sosnick, T.; Freed, K. *Biochemistry* **2005**, *44*, 9691−9702.
(40) Scholtz, J.; York, E.; Stewart, J.; Baldwin, R. *J. Am. Chem. Soc.* **1991**, *113*, 5102−5104.
(41) Shalongo, W.; Dugad, L.; Stellwagen, E. *J. Am. Chem. Soc.* **1994**, *116*, 8288−8293.
(42) David, A.; Scheurer, C.; Bruschweiler, R. *J. Am. Chem. Soc.* **2000**, *122*, 10390−10397.
(43) Schmidt, J.; Blümel, M.; Löhr, F.; Rüterjans, H. *J. Biomol. NMR* **1999**, *14*, 1−12.
(44) Neal, S.; Nip, A. M.; Zhang, H.; Wishart, D. S. *J. Biomol. NMR* **2003**, *26*, 215−240.
(45) Frishman, D.; Argos, P. *Proteins* **1995**, *23*, 566−579.
(46) Case, D.; Darden, T.; Cheatham, T., III; Simmerling, C.; Wang, J.; Duke, R.; Luo, R.; Crowley, M.; Walker, R.; Zhang, W.; et al. University of California: San Francisco, 2008, p 32.
(47) Wang, A. C.; Bax, A. *J. Am. Chem. Soc.* **1995**, *117*, 1810−1813.